Proc. Natl. Acad. Sci. USA
Vol. 96, pp. 2919–2924, March 1999
Genetics

Different *TBX5* interactions in heart and limb defined by Holt–Oram syndrome mutations

CRAIG T. BASSON*, TAOSHENG HUANG†, ROBERT C. LIN†, DAVID R. BACHINSKY†, STANISLAWA WEREMOWICZ‡, ALICIA VAGLIO§, RINA BRUZZONE§, ROBERTO QUADRELLI§, MARGHERITA LERONE¶, GIOVANNI ROMEO¶, MARGHERITA SILENGO¶, ALEXANDRE PEREIRA‖, JOSE KRIEGER‖, SONIA F. MESQUITA‖, MITSUHIRO KAMISAGO§§, CYNTHIA C. MORTON‡**, MARY ELLA M. PIERPONT††, CHISTOPH W. MÜLLER‡‡, J. G. SEIDMAN†, AND CHRISTINE E. SEIDMAN§§¶¶

*Cardiology Division, Department of Medicine and Department of Cell Biology and Anatomy, Weill Medical College of Cornell University, The New York Hospital, New York, NY 10021; †Department of Genetics, Howard Hughes Medical Institute, Harvard Medical School, Boston, MA 02115; ‡Department of Pathology, Brigham and Women's Hospital and Harvard Medical School, Boston, MA 02115; §Instituto de Genetica Medica, Hospital Italiano, Montevideo, Uruguay; ¶Laboratorio de Genetica Molecolare, Instituto Giannina Gaslini, Genoa, Italy; ‖Instituto Do Coraçao, Univercidade de Sao Paulo, Brazil 01060-970; **Department of Obstetrics, Gynecology and Reproductive Biology, Brigham and Women's Hospital, Boston, MA 02115; ††Ray and Hattie Anderson Center for the Study of Hereditary Cardiac Disease, Department of Pediatrics, University of Minnesota, Minneapolis, MN 55455; ‡‡European Molecular Biology Laboratory, Grenoble Outstation, c/o ILL BP 156, 38042 Grenoble Cedex 9, France; §§Howard Hughes Medical Institute, Cardiovascular Division, Department of Medicine, Brigham and Women's Hospital, Harvard Medical School, Boston, MA 02115

Communicated by Philip Leder, Harvard Medical School, Boston, MA, January 11, 1999 (received for review October 21, 1998)

ABSTRACT **To better understand the role of TBX5, a T-box containing transcription factor in forelimb and heart development, we have studied the clinical features of Holt–Oram syndrome caused by 10 different *TBX5* mutations. Defects predicted to create null alleles caused substantial abnormalities both in limb and heart. In contrast, missense mutations produced distinct phenotypes: Gly80Arg caused significant cardiac malformations but only minor skeletal abnormalities; and Arg237Gln and Arg237Trp caused extensive upper limb malformations but less significant cardiac abnormalities. Amino acids altered by missense mutations were located on the three-dimensional structure of a related T-box transcription factor, *Xbra*, bound to DNA. Residue 80 is highly conserved within T-box sequences that interact with the major groove of target DNA; residue 237 is located in the T-box domain that selectively binds to the minor groove of DNA. These structural data, taken together with the predominant cardiac or skeletal phenotype produced by each missense mutation, suggest that organ-specific gene activation by TBX5 is predicated on biophysical interactions with different target DNA sequences.**

T-box genes encode transcription factors that contain a highly conserved DNA binding motif (T-box or T-domain) composed of ≈180 amino acid residues (1, 2). Members of this gene family have been found in vertebrates (e.g., *Xbra* and *Eomesodermin* in *Xenopus laevis*) and invertebrates (e.g., *optomotor blind* (*omb*) in *Drosophila melanogaster*). The mouse and human genomes each contain at least seven T-box gene family members including *T, TBr, TBX2, TBX3, TBX4, TBX5*, and *TBX6* (1–4). The three-dimensional structure of the T-box–DNA complex has recently been elucidated by analyses of the *Xbra* T-box bound to a 24-nt palindrome duplex (5). These studies demonstrated that *Xbra*, and presumably other T-box transcription factors, bind to their target DNAs as homodimers which interact with both major and minor grooves of their DNA targets (5).

Analyses of the phenotypes produced by T-box gene mutations have elucidated some of the functions of these proteins (6, 7). Studies of murine *Brachyury* mutations (insertions or deletions in *T*) implicate a critical role for the T-protein in tissue specification, morphogenesis and organogenesis (7, 8). *D. melanogaster omb* phenotypes have shown that T-box proteins participate in axis formation, particularly during development of distal wing structures (9). Mutations in two human T-box genes have also recently been demonstrated to cause disease (10–12). *TBX3* defects cause the autosomal dominant condition ulnar-mammary syndrome (OMIM 181450; http://www.ncbi.nlm.nih.gov/omim/; ref. 13), a disorder characterized by abnormalities in posterior upper limb structures, apocrine/mammary glands, teeth, and genital–urinary tract, thereby identifying this T-box protein as a participant in ectoderm–mesoderm inductive processes (12). Mutations in *TBX5* cause autosomal dominant Holt–Oram syndrome (OMIM 142900; ref. 13), a rare condition (1/100,000 live births) characterized by anterior pre-axial limb and cardiac malformations (10, 11). Although Holt–Oram syndrome is a highly penetrant disorder, clinical manifestations vary substantially (13–24). All affected individuals exhibit upper limb radial ray malformations that range from subtle carpal bone abnormalities to overt proximal defects such as phocomelia; many also have congenital heart disease. Cardiac defects can be isolated ostium secundum atrial septal defects (ASD) or muscular ventricular septal defects (VSD), or multiple and complex malformations. The mechanism by which mutations in a single T-box gene can affect these disparate organ systems remains uncertain.

To further understand the role of *TBX5* in human morphogenesis, we have identified mutations that cause Holt–Oram syndrome and have defined the clinical phenotypes produced by these mutations. Some of the mutations are predicted to function as null alleles, whereas others are missense mutations that appear to encode active, mutant protein. We demonstrate a correlation between the locations of the missense mutations and associated clinical phenotypes. An amino acid alteration near the amino-terminal end of the T-box, which should affect interactions with the major groove of the target DNA sequence, produces very significant cardiac malformations. In contrast, amino acid changes at the carboxyl end of the T-box, which should affect interactions between TBX5 and the minor groove of the DNA target sequence, produce severe limb

The publication costs of this article were defrayed in part by page charge payment. This article must therefore be hereby marked "*advertisement*" in accordance with 18 U.S.C. §1734 solely to indicate this fact.

PNAS is available online at www.pnas.org.

Abbreviation: FISH, fluorescence *in situ* hybridization analysis.

The sequence reported in this paper has been deposited in the GenBank database (accession nos. U80987 and U89353).

A Commentary on this article begins on page 2577.

¶¶To whom reprint requests should be addressed at: Department of Genetics, Harvard Medical School, Alpert 533, 200 Longwood Avenue, Boston, MA 02115. e-mail: cseidman@rascal.med.harvard.edu.

abnormalities. These findings imply that structurally distinct TBX5–target DNA interactions have different functional consequences in the developmental pathways of limb and heart morphogenesis.

MATERIALS AND METHODS

Clinical Evaluations. Informed consent was obtained from all participants in accordance with the Brigham and Women's Hospital Human Research Committee. Clinical evaluations were obtained without prior knowledge of genotype status. Holt–Oram syndrome probands and first-degree family members were evaluated by history and physical examination, radiographic studies of hands, electrocardiography, and transthoracic echocardiography with color-flow Doppler. Individuals with evidence of radial ray skeletal abnormalities were considered affected by Holt–Oram syndrome if they or at least one family member also had congenital cardiac defects or conduction disease. Clinical evaluations of families A, B, and F have been reported previously (15, 25).

Clinical data from all available individuals with a *TBX5* mutation were compared between families and analyzed by using the χ^2 test. "Severe" skeletal malformation was defined as phocomelia or marked ectromelia involving both the radius and humerus as described (15). "Composite" cardiac malformations indicate multiple septation defects, a single septation defect in the setting of other cardiovascular anomalies, or complex congenital heart disease. Clinical data on individuals with the Arg279ter and the InsSer387FSter mutations, expected to cause carboxyl-terminal truncation of TBX5 (11), were not available.

DNA Isolation. Five to 30 ml of peripheral blood was obtained from each family member. DNA was isolated from peripheral lymphocytes or lymphoblastoid cell lines (15) by digestion with Proteinase K and phenol-chloroform purification as described (15).

***TBX5* Gene Sequence Analysis and Mutation Identification.** To identify *TBX5* mutations, all exons (exons 2–9) encoding the polypeptide were sequenced in samples from Holt–Oram syndrome probands. Exons 2–8 were amplified by the PCR by using previously described primers (10). Exon 9 was amplified with primers 9GF, 5′-TACTTTGGACAATATACTGTCTCC-3′ and 9GR, 5′-CGACCTTGAGTGCAGAATGTGAAC-3′. PCR conditions used were 94°C for 20 s, 60°C for 30 s, and 72°C for 45 s for 35 cycles. PCR products were then purified by using QIAquick columns per the manufacturer's protocol (Qiagen, Chatsworth, CA). Templates were subjected to cycle sequencing by using ^{32}P end-labeled forward and reverse primers, as described (10), or were sequenced by using fluoresceinated dideoxynucleotides and analyzed on an Applied Biosystems 377 automated DNA sequencer.

Each nucleotide sequence alteration detected by DNA sequence analysis was confirmed by an alternate procedure. The Glu69ter mutation was confirmed by digestion of PCR amplified DNA with *Dde*I as described (10). The Gly80Arg (family A), InsMet83FSter (family IIq) and ΔAsp140FSter (family IId) mutations were independently confirmed by restriction enzyme digestion analyses, as follows: (*i*) Gly80Arg, exon 3 was amplified by PCR from DNA derived from family members or unrelated individuals by using primers 3GF and 3GR (10); PCR products were digested with *Bfa*I; (*ii*) InsMet83FSter, exon 4 was PCR amplified from an affected individual's DNA and then digested with *Aci*I; digested products were analyzed on a 3% NuSieve/1% agarose nondenaturing gel; (*iii*) ΔAsp140FSter, exon 4 was PCR amplified from an individual's DNA (10) and then digested with *Bgl*I; digested products were analyzed on a 3% NuSieve/1% agarose nondenaturing gel.

Five mutations (Ser196ter, family IIb; ΔGlu243FSter, family E; Arg237Trp, family V; Int2ASC$_{-2}$A, family IIj; Int2ASG$_{+1}$C, family III) were independently confirmed by using allele-specific oligonucleotide hybridization as described (26). To detect mutations Int2ASG$_{+1}$C, Int2ASC$_{-2}$A, Ser196ter, ΔGlu243FSter, and Arg237Trp, exons 3, 6 and 7 were PCR-amplified from DNA derived from family members and unrelated individuals with primer pairs 3GF/3GR, 6GF/6GR, or

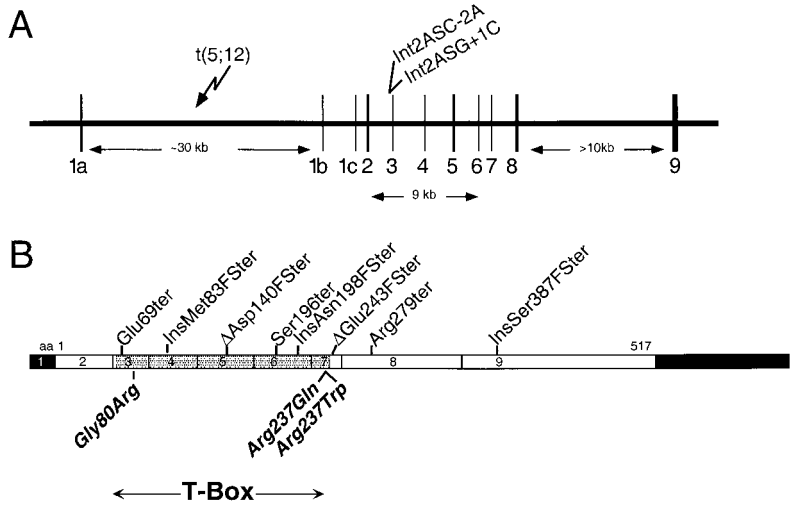

FIG. 1. Fourteen mutations in *TBX5* that cause Holt–Oram syndrome. (*A*) *TBX5* genomic structure (our unpublished data and refs. 10 and 11) is shown with approximate intron sizes. Exons 1–9 are shown with vertical bars. Exons 1a, 1b, or 1c are alternatively spliced as the first exon of the *TBX5* cDNA. Alternative splicing of the 3′ region of the gene accounts for the variable addition of exon 9. Arrows indicate the translocation t(5;12)(q15;q24) found in the family IIa proband [designated t(5;12)], which disrupts *TBX5* in intron 1a and the location of intron 2 acceptor site (AS) mutations Int2ASC$_{-2}$A and Int2ASG$_{+1}$C. Acceptor site residues were numbered from the splice site with the conserved G residue designated as +1. (*B*) Schematic representation of *TBX5* cDNA (GenBank accession nos. U80987 and U89353) illustrating the largest of the alternatively spliced transcripts. Untranslated sequence (dark shading), exons 1–9 (numbered boxes), and locations of amino acids 1 and 517 are indicated. Codons (gray shading) that encode the T-box DNA binding domain [residues 56–238 (exons 3–7)] were defined by homology to other T-box gene family members. *TBX5* mutations that are predicted to truncate TBX5 are shown above; missense mutations are indicated below (bold, italics). Mutations are designated by the name and number of the first substituted amino acid residue: Δ, deletion; Ins, insertion. FSter indicates frameshift mutations with resultant premature stop codons; ter indicates nonsense mutation. Mutations Glu69ter, Arg237Gln, InsAsn198FSter, Arg279ter, and InsSer387FSter have been described (10, 11). Mutation Ser196ter, reported here, was also previously observed in an unrelated family (11).

Table 1. TBX5 mutations detected in individuals affected by Holt–Oram syndrome

Family	Designation*	Nucleotide change		Class of Mutation	Ref.
		Mutation	Residue no.		
A	Gly80Arg	G → A	238	Missense	See text
B	Arg237Gln	G → A	710	Missense	10
IIg	Arg237Gln	G → A	710	Missense	
V	Arg237Trp	C → T	709	Missense	See text
E	ΔGlu243FSter	G deletion	727	Frameshift; truncated at codon 263	See text
F	Glu69ter	G → T	205	Nonsense; truncated at codon 69	10
IIa	t(5;12)(q15;q24)			Intron 1A disruption; translocation	See text
IIb	Ser196ter	C → A	587	Nonsense; truncated at codon 196	See text; 11
IId	ΔAsp140FSter	13-bp deletion	420–432	Frameshift; truncated at codon 145	See text
IIj	Int2ASC$_{-2}$A	C$_{-2}$ → A in Intron 2 acceptor site		Intron 2 splice acceptor site mutation; truncation	See text
II1	Int2ASG$_{+1}$C	G$_{+1}$ → C in intron 2 acceptor site		Intron 2 splice acceptor site mutation; truncation	See text
IIq	InsMet83FSter	G → AA	246	Frameshift; truncated at codon 94	See text

*The location of mutations in the *TBX5* gene is indicated in Fig. 1. Amino acid residues are numbered as described (10). IIj and II1 are splice acceptor site (AS) mutations; the nucleotides are numbered as described (10).

7GF/7GR, respectively (10). PCR products were purified over QIAquick columns, and 10 ng of product was applied to GenescreenPlus (New England Nuclear) nylon membranes by using a slot-blot apparatus. Membranes were hybridized to ^{32}P end-labeled oligonucleotides representing normal or mutant (italicized) sequences as follows: Ser196ter, normal, 5′-ATTTGGCTCAAAAAATA-3′ and mutant, 5′-ATTTGGCT*A*AAAAAATA-3′; ΔGlu243FSter, normal, 5′-ATGACATGGAGCTGCAC-3′ and mutant, 5′-ATGACAT*G*AGCTGCAC-3′; Arg237Trp, normal, 5′-AGGATTTCGGGGCAGTG-3′ and mutant, 5′-AGGATTT*T*GGGGCAGTG-3′; Int2ASG$_{+1}$C, normal, 5′-TTCTTGCAGGGCATGGA-3′ and mutant, 5′-TTCTTGCA*C*GGCATGGA-3′; Int2ASC$_{-2}$A, normal, 5′-CCTTCTTGCAGGGCATG-3′ and mutant, 5′-CCTTCTTG-*A*AGGGCATG-3′. Membranes were then washed, and the radioactive signal was quantitated as described (10, 26).

Mutation Arg237Gln (family IIg) was confirmed by amplification refractive mutation specific (ARMS) PCR as described (27) by using oligonucleotide primers CCATGTCATCACTGCCCT and 7GF (10). The Arg237Gln mutation in members of family B was confirmed by allele specific hybridization as described (10).

Fluorescence *in Situ* Hybridization Analysis (FISH). Metaphase chromosomes were prepared from lymphoblastoid cell lines derived from the affected individual in family IIa and studied by FISH analysis by using a *TBX5* cDNA probe (TBX5.4; ref. 10) and a *TBX5* genomic clone (JE98). Probes were labeled as described (28) with digoxigenin-11-dUTP and hybridized to metaphase chromosome preparations. Digoxigenin-labeled probe was detected with rhodamine-labeled antidigoxigenin Ab, and metaphase chromosomes were counterstained with 4,6-diamidino-2-phenylindoledihydrochloride (DAPI). More than 20 metaphase preparations were examined for fluorescent signal for each probe.

RESULTS

Genetic Studies. *TBX5* sequences of exons 2–9 and flanking splice signals were ascertained (see *Materials and Methods*) in unrelated probands with Holt–Oram syndrome. Ten sequence variants (Fig. 1) were identified in 11 probands that are predicted to alter the encoded protein [Table 1; mutations in families B and F have been previously reported (10)]. Although *TBX5* sequences encoding protein were normal in the affected individual (Fig. 2) from family IIa, a metaphase karyotype revealed a translocation with a breakpoint at chromosome 12q24 [46,XX, t(5;12)(q15;q24)]. Southern blot analyses excluded rearrangements between exons 1b and 8. To determine whether the translocation disrupted 5′ alternatively spliced exons (Fig. 1) or 3′ regions, FISH analyses of metaphase chromosomes were performed by using a 5′ probe (clone JE98, containing exon 1a and flanking intron sequences) and a 3′ probe (cDNA clone TBX5.4). Probe TBX5.4 hybridized to both the normal and derivative chromosome 12 (Fig. 2*C*), whereas probe JE98 (Fig. 2*D*) hybridized to the normal chromosome 12 and the derivative chromosome 5. The translocation thus disrupts the *TBX5* gene in the intron following exon 1a, thereby separating protein-encoding exons 2–9 from promoter elements and 5′ untranslated sequences.

These *TBX5* sequence variants (Table 1) were considered mutations based on their cosegregation with disease status in study families, their absence in more than 100 chromosomes derived from unrelated normal subjects, and the significant change each was predicted to cause in TBX5 structure or

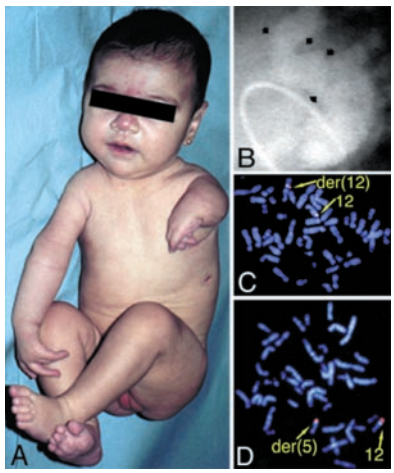

FIG. 2. A chromosome 5;12 translocation causes severe skeletal and composite cardiac malformations. (*A*) The affected child in family IIa has left arm phocomelia, right radial hypoplasia, and right thumb aplasia. (*B*) Cardiac angiography demonstrated a common atrium and a complete atrioventricular canal defect. Contrast dye injected from a catheter passed across the atrioventricular septal defect from the right to left ventricle reveals a marked deformity (arrowheads, characteristic of this malformation. (*C* and *D*) FISH analysis of metaphase chromosomes from the affected child in family IIa demonstrates a breakpoint in the intron following exon 1a of *TBX5*. Pink signal indicates hybridization of *TBX5*.4 cDNA (encoding protein sequence) to a normal and derivative chromosome 12 in *C*. Hybridization of a genomic clone (JE98) containing exon 1a (*D*) produced pink signal in a normal chromosome 12 and the derivative chromosome 5.

levels. Two families shared an Arg237Gln missense mutation; haplotype analyses indicated this defect arose independently in each (data not shown). Moreover, five *de novo* mutations arose in Holt–Oram probands (E, IIa, IIb, III, or IId); parents of these individuals had neither clinical evidence of Holt–Oram syndrome nor the disease-causing mutation. Family IIb demonstrated this *de novo* mutation to be a germ-line defect, which was transmitted to affected offspring.

Seven mutations (Glu69ter, InsMet83FSter, Ser196ter, ΔAsp140FSter, Int2ASC$_{-2}$A, Int2ASG$_{+1}$C, and ΔGlu243FSter) should encode markedly truncated TBX5 derivatives that lack T-box sequences involved in DNA binding (29, 30) and presumably cannot activate transcription. These defects and the t(5;12)(q15;q24) translocation therefore appear to function as null alleles.

Three missense mutations, Gly80Arg, Arg237Trp, and Arg237Gln, that alter a single amino acid in T-box sequences were identified in four families. As a first step toward predicting the consequences of these mutations, each was mapped onto the three-dimensional structure of the *Xbra* T-box, bound with target DNA (5). Amino acids encoded in the T-box domain of human *TBX5* and *X. laevis Xbra* are 54% identical and 74% homologous (Fig. 3 and ref. 5), suggesting that the three-dimensional structures of these DNA binding domains are likely to be similar.

Crystallographic structure data indicate that the T-box interacts with both the major and minor groove of target DNA (5). The Gly80Arg mutation occurs near the amino-terminal end of the T-box, designated the *ab*-loop (5), and follows an α-helix. An adjacent arginine residue (human residue 81; *X. laevis* residue 67; Fig. 3) forms two hydrogen bonds with target DNA (guanine residue 5) and contacts the phosphate backbone in the major groove (5). Replacement of glycine residue 80 by arginine should therefore alter the *ab*-loop structure and potentially impair interactions with the major groove of target DNA.

Arginine residue 237, located at the carboxyl end of human T-box sequences, is highly conserved in many T-box genes. The comparable *Xbra* residue (amino acid 216) is leucine, which abuts the hydrophobic portion of lysine residue 207 (5). Folding of human TBX5 would position arginine residue 237 near glutamate residue 228 and favor formation of a salt bridge. Substitution of either glutamine (a polar residue) or tryptophan (hydrophobic) for arginine at residue 237 would probably break this salt bridge and restructure the terminal T-box helix. Because this carboxyl helix interacts with the minor groove of target DNA, we expect that the Arg237Trp and Arg237Gln mutations specifically alter TBX5 interaction with target DNA.

Clinical Manifestations of *TBX5* Mutations. The clinical features of Holt–Oram syndrome in all probands and their affected relatives (Table 2) confirmed previous descriptions (13–24) of this syndrome: all had upper limb malformations and 76% also had congenital cardiac malformations. However


```
                 .         .    R    .         .         .         .         .         .         .
Hum VFLHERELWLKFHEVGTEMIITKAGRRMFPSYKVKVTGLNPKTKYILLMDIVPADDHRYKFADNKWSVTGKAEPAMPGRLYVHPDSPATGAHWMRQLVSF 155
    | |.||:|| :|.|:..|||:||.|||||| .||.:.||:|...|.:|:|:|:||:||:|:.:..| ..||:||. |: :|:|||||. ||||||:: |||
XLe VSLEERDLWTRFKELTNEMIVTKNGRRMFPVLKVSMSGLDPNAMYTVLLDFVAADNHRWKYVNGEWVPGGKPEPQAPSCVYIHPDSPNFGAHWMKDPVSF 100

                 .         .         .         .         .         .         .    Q
Hum QKLKLTNNHLDPFGHIILNSMHKYQPRLHIVKADENNGFGSKNTAFCTHVFPETAFIAVTSYQNHKITQLKIENNPFAKGFRG                238
    ¦:||||. ::. ¦:|:|||:|||:||:|||:       .|:..  :..¦ ||||.|||||.|||..||.|||.:||||||:| :
XLe SKVKLTNK.MNGGGQIMLNSLHKYEPRIHIVR......VGGTQRMITSHSFPETQFIAVTAYQNEEITALKIKHNPFAKAFLD                217
```

FIG. 3. (*Upper*) Three-dimensional structure of the *X. laevis Xbra* T-box bound to a 24-nt DNA duplex indicating the location of residues Gly-80 (red) and Arg-237 (yellow) mutated in the missense mutations Gly80Arg, Arg237Gln, and Arg237Trp. Note that the T-box binds its target DNA (teal and blue) as a homodimer. (*Lower*) Human *TBX5* and *X. laevis Xbra* T-box sequences are aligned. The Gly80Arg (R) and Arg237Gln (Q) missense mutations are located in the T-box sequence. A vertical line indicates identical sequences in *Xbra* and *TBX5*, two dots indicate functionally related residues, and one dot denotes nonconserved residues.

Table 2. Incidence of congenital cardiovascular and skeletal malformations in individuals with Holt–Oram syndrome causing TBX5 mutations

Class of mutation	Amino acid residues	Families	No. of Individuals	All cardiac malform.	All skeletal malform.	Composite cardiac malform.	Severe skeletal malform.
Truncation		E, F, IIa, IIb, IId, IIj, II1, IIq	26	21	26	16	18
Missense	80	A	19	19	19	4	0
Missense	237	B, IIg, V	26	14	26	1	9

Malform., malformations.

significant differences were observed in the expression of limb or cardiac phenotype (see *Materials and Methods*) resulting from distinct *TBX5* defects (Table 2). We assumed that the mutations creating truncated forms of TBX5 encoded "null alleles" and therefore these individuals were treated as a single class. Sixty-five percent of individuals with TBX5 haploinsufficiency (resulting from a TBX5 truncation mutation or null allele) had severe skeletal malformations, and 57% of these individuals had composite cardiac malformations.

The incidence and severity of Holt–Oram limb and heart malformations caused by *TBX5* missense mutations depended on the specific amino acid residue altered (Table 2). The incidence of composite cardiac malformation caused by the Gly80Arg mutation was 21%, not significantly different from the incidence of composite cardiac malformation caused by TBX5 haploinsufficiency. In contrast, individuals with the Gly80Arg mutation had only mild carpal bone and thumb deformities, but a significantly lower incidence of severe skeletal malformation than that caused by *TBX5* haploinsufficiency ($P < 0.0001$). Missense mutations Arg237Gln or Arg237Trp caused severe skeletal malformations in 35% of affected individuals, comparable to the incidence of severe skeletal malformations caused by haploinsufficiency. However, significantly more severe skeletal malformations were observed in individuals with the Arg237Gln and Arg237Trp missense mutations than in individuals with the Gly80Arg missense mutation ($P = 0.004$). Composite cardiac malformations (4%) occurred less frequently in individuals with an Arg-237 missense mutation than mutations producing *TBX5* haploinsufficiency ($P < 0.0001$) or the Gly80Arg missense mutation.

DISCUSSION

Genetic data indicate that the limb and cardiac malformations that characterize Holt–Oram syndrome can be produced by nonsense mutations, deletions, rearrangements, and missense mutations in the *TBX5* gene. Insertions in the *TBX5* gene have also been reported (11). Studies of families III, IIb, IId, E, and IIa and a previous report (11) indicate *de novo* mutations are prevalent in Holt–Oram syndrome. Given this observation and the low incidence of the disease (1/100,000 live births), it was surprising that three *TBX5* residues are mutated in multiple families [Ser-196 (families IIb and ref. 11)], Arg-279 (11), and Arg-237 (families IIg, B, V)]. These findings may indicate greater susceptibility of particular *TBX5* nucleotides to mutation. Alternatively, mutation of certain residues may produce a more pronounced and easily recognized phenotype.

The majority of *TBX5* mutations introduce premature stop codons (Table 1) that are predicted to encode markedly truncated polypeptides. Even if mutant species were stable in the cell, foreshortened TBX5 molecules are unlikely to maintain full integrity of the T-box. Analyses of T-box function in the related *T* (*Brachyury*) gene have demonstrated that even minimal truncation of this domain eliminates DNA binding capacity (29). Hence, truncation mutations in the T-box and gene disruption (i.e., chromosome 5;12 translocation) probably cause haploinsufficiency of T-box activity. The carboxyl region of the murine T-box gene, *T,* has recently been demonstrated to regulate transcriptional activity (30); a comparable domain in *TBX5* should be perturbed by truncation mutations. The marked similarities in clinical phenotype (severe skeletal and composite cardiac malformations) of Holt–Oram syndrome caused by multiple, different truncation defects or a null allele indicate that precise regulation of *TBX5* concentration is required for the physiologic expression of critical genes during the development of these structures.

Analyses of the consequences of rare *TBX5* missense mutations (Gly80Arg, Arg237Gln, and Arg237Trp) are perhaps more instructive of the roles that this transcription factor plays during embryogenesis. Because these mutations encode only a single amino acid substitution, they are less likely to cause transcript or peptide instability. We propose that these gene defects function through a dominant-negative mechanism rather than through haploinsufficiency. This hypothesis is supported and extended by considerations of the probable biophysical consequences of missense mutations, based on recent crystallographic structure of *X. laevis Xbra* bound to its DNA target (5) and analyses of the distinct clinical phenotypes associated with human *TBX5* mutations. The T-box binds DNA as a homodimer; hence heterozygote alleles in affected individuals could produce three possible *TBX5*–target DNA interactions (wild type, mutant/wild type, mutant). We suspect that diversity in dimer formation contributes to phenotypic variability in individuals with the same mutation. Phenotypic variability also appears to be influenced by the location of a mutation within TBX5. Before the identification of *TBX5* as the disease gene, clinical studies recognized a disparity in the Holt–Oram phenotype in two large kindreds (predominance of composite cardiac defects in family A versus severe skeletal malformations in family B [15]). Surprisingly, these two families have TBX5 missense mutations that are predicted to alter residues with distinct target DNA interactions. The missense mutation in family A (Gly80Arg) should perturb *TBX5* binding to the major groove of the target DNA, whereas the defect in family B (Arg237Gln) should perturb *TBX5* interactions with the minor groove of target DNA (Fig. 3). Clinical findings comparable to those in family B were found in affected individuals from two other, unrelated families (IIg, V), whose mutations also alter TBX5 residue 237. Although other models are possible, collectively these data suggest the hypothesis that critical *TBX5* interactions with target DNA are different in developing heart and limb.

TBX5, and its associated transcriptional cofactors, might activate identical genes in the developmental pathways of heart and limb; however, a simple explanation of the data presented here is that TBX5, directly or indirectly, alters the transcription of different genes in heart and limb. Presumably, unknown TBX5-interacting proteins expressed in these tissues influences TBX5 binding to target DNA sequences. Further analyses of structure-function relationship of *TBX5* and the identification of genes activated by this transcription factor should help to elucidate the signals that delineate development of these organs.

We are grateful to the family members and physicians (Drs. Lewis Holmes, Aaron Stern, Andrew Poznanski, Barbara Weissman, and Scott Solomon) who participated in these studies. We also thank Mr. Mohammed Miri, Ms. Tatjana Levi, Mr. Johann Soults, and Ms. Barbara McDonough for technical assistance. This work was supported by National Institutes of Health Grant HL03468 (C.T.B.) and the Howard Hughes Medical Institute (D.R.B., J.G.S., and C.E.S.).

1. Bollag, R. J., Siegfried, Z., Cebra-Thomas, J. A., Garvey, N., Davison, E. M. & Silver, L. M. (1994) *Nat. Genet.* **7,** 383–389.
2. Holland, P. W., Koschorz, B., Holland, L. Z. & Herrmann, B. G. (1995) *Development (Cambridge, UK)* **121,** 4283–4291.
3. Agulnik, S. I., Garvey, N., Hancock, S., Ruvinsky, I., Chapman, D. L., Agulnik I., Bollag R., Papaioannou, V. & Silver, L. M. (1996) *Genetics* **144,** 249–254.
4. Agulnik, S. I., Ruvinsky, I. & Silver, L. M. (1997) *Genome* **40,** 458–464.
5. Muller, C. W. & Herrmann, B. G. (1997) *Nature (London)* **389,** 884–888.
6. Meisler, M. H. (1997) *Mamm. Genome* **8,** 799–800.
7. Kavka, A. I. & Green, J. B. (1997) *Biochi. Biophys. Acta* **1333,** F73–F84.
8. Smith, J. (1997) *Curr. Opin. Genet. Dev.* **7,** 474–480.
9. Kopp, A. & Duncan I. (1997) *Development (Cambridge, UK)* **124,** 3715–3726.
10. Basson, C. T., Bachinsky, D. R., Lin, R. C., Levi, T., Elkins, J. A., Soults, J., Grayzel, D., Kroumpouzou, E., Traill, T. A., Leblanc-Straceski, J., *et al*. (1997) *Nat. Genet.* **15,** 30–35.
11. Li, Q. Y., Newbury-Ecob, R. A., Terrett, J. A., Wilson, D. I., Curtis, A. R., Yi, C. H., Gebuhr, T., Bullen, P. J., Robson, S. C., Strachan, T., *et al*. (1997) *Nat. Genet.* **15,** 21–29.
12. Bamshad, M., Lin, R. C., Law, D. J., Watkins, W. S., Krakowiak, P. A., Moore, M. E., Franceshinin, P., Lala, R., Holmes, L. B., Gebuhr, T. C., *et al*. (1997) *Nat. Genet.* **16,** 311–315.
13. Online Mendelian Inheritance in Man, OMIM, Johns Hopkins University, Baltimore, MD.
14. Leck, I. (1993) in *Human Malformations and Related Anomalies.* Stevenson, R. E., Hall, J. G. & Goodman, M. M., eds. (Oxford Univ. Press, Oxford), Vol. 1, pp. 65–94.
15. Basson, C. T., Cowley, G. S., Traill, T. A., Solomon, S., Seidman, J. G. & Seidman, C. E. (1994) *N. Engl. J. Med.* **330,** 885–891.
16. Csaba, E., Marta, V. & Czeizel, E. (1991) *Orvosi. Hetilap.* **132,** 73–78.
17. Hurst, J. A., Hall, C. M. & Baraitser, M. (1991) *J. Med. Genet.* **28,** 406–410.
18. Holt, M. & Oram, S. (1960) *Br. Heart. J.* **22,** 236–242.
18. Poznanski, A. K., Gall, J. C. & Stern, A. M. (1970) *Radiology* **94,** 45–53.
20. Smith, A. T., Sack, G. H. & Taylor, G. J. (1979) *J. Pediatr.* **95,** 538–543.
21. Gall, J. C., Stern, A. M., Cohen, M. M., Adams, M. S. & Davidson, R. T. (1966) *Am. J. Hum. Genet.* **18,** 187–200.
22. Kullman, F. & Grimm, T. (1993) *Dtsch. Med. Wochenschr.* **118,** 1455–1462.
23. Letts, R. M., Chudley, A. E., Cumming, G. & Shokier, M. H. (1976) *Clin. Orthop. Relat. Res.* **116,** 149–154.
24. Pruznanski, W. (1964) *Cardiologia* **45,** 1–38.
25. Basson, C. T., Solomon, S. D., Weissman, B., MacRae, C. A., Poznanski, A. K., Prieto, F., de la Fuente, S. R., Pease, W. E., Levin, S. E., Holmes, L., *et al*. (1995) *Circulation* **91,** 1326–1329.
26. Benson, D. W., MacRae, C. A., Vesely, M. R., Walsh, E. P., Seidman, J. G., Seidman, C. E. & Satler, C. A. (1996) *Circulation* **93,** 1791–1795.
27. Newton, C. R., Graham, A., Heptinstall, L. E., *et al*. (1989) *Nucleic Acids Res.* **17,** 2503–2516.
28. Zhao, Y., Bjorbaek, C., Weremowicz, S., Morton, C. C. & Moller, D. E. (1995) *Mol. Cell. Biol.* **15,** 4353–4363.
29. Kispert, A. & Herrmann, B. G. (1993) *EMBO J.* **12,** 3211–3220.
30. Kispert, A., Koschorz, B. & Herrmann, B. G. (1995) *EMBO J.* **14,** 4763–4772.